ACS NANO
Cite This: ACS Nano XXXX, XXX, XXX−XXX
www.acsnano.org

ARTICLE

Confined 1D Propulsion of Metallodielectric Janus Micromotors on Microelectrodes under Alternating Current Electric Fields

Liangliang Zhang,[†,§] Zuyao Xiao,[†,§] Xi Chen,[†] Jingyuan Chen,[†] and Wei Wang*[,†,‡]

[†]School of Materials Science and Engineering, Harbin Institute of Technology (Shenzhen), Shenzhen, Guangdong 518055, China
[‡]IBS Center for Soft and Living Matter, Institute of Basic Science, Ulsan 44919, Republic of Korea

Supporting Information

ABSTRACT: There is mounting interest in synthetic microswimmers ("micromotors") as microrobots as well as a model system for the study of active matters, and spatial navigation is critical for their success. Current navigational technologies mostly rely on magnetic steering or guiding with physical boundaries, yet limitations with these strategies are plenty. Inspired by an earlier work with magnetic domains on a garnet film as predefined tracks, we present an interdigitated microelectrodes (IDE) system where, upon the application of AC electric fields, metallodielectric (e.g., SiO_2−Ti) Janus particles are hydrodynamically confined and electrokinetically propelled in one dimension along the electrode center lines with tunable speeds. In addition, comoving micromotors moved in single files, while those moving in opposite directions primarily reoriented and moved past each other. At high particle densities, turbulence-like aggregates formed as many-body interactions became complicated. Furthermore, a micromotor made U-turns when approaching an electrode closure, while it gradually slowed down at the electrode opening and was collected in large piles. Labyrinth patterns made of serpentine chains of Janus particles emerged by modifying the electrode configuration. Most of these observations can be qualitatively understood by a combination of electroosmotic flows pointing inward to the electrodes, and asymmetric electrical polarization of the Janus particles under an AC electric field. Emerging from these observations is a strategy that not only powers and confines micromotors on prefabricated tracks in a contactless, on-demand manner, but is also capable of concentrating active particles at predefined locations. These features could prove useful for designing tunable tracks that steer synthetic microrobots, as well as to enable the study of single file diffusion, active turbulence, and other collective behaviors of active matters.

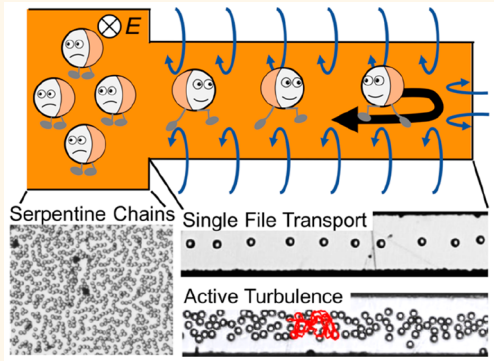

KEYWORDS: *interdigitated microelectrodes, ICEP, electroosmosis, hydrodynamic trapping, micromotors, active colloids*

Over the recent years, research on synthetic microswimmers ("micromotors") have attracted mounting attention.[1−12] They convert external energy stored in the environment into motion in liquid and move in a way similar to microorganisms such as bacteria and algae.[13] These biomimetic microparticles are thus expected to find uses in applications ranging from sensing to drug deliveries.[14] In addition, their mimicry to biological microswimmers makes them promising model systems for the study of active matters,[15−17] an interdisciplinary research field that is rapidly advancing.

Whether used for practical applications or as model systems for fundamental studies, strategies for controlling the locations and orientations of a synthetic microswimmer is crucial for the task.[18−21] Most of existing techniques of spatial controls of a microswimmer fall into three categories. The first category of technique uses magnetic fields to actively steer a magnetic microswimmer.[22−24] This often requires complicated magnetic setups such as Helmholtz coils and particles being steered need to be magnetic. In addition, constant interference, whether manual or automatic, is also required. The second method constructs physical boundaries, such as microchannels or microstructures, along which microswimmers preferably move.[25−28] This often requires complicated microfabrication process such as lithography, and swimmer-wall interaction is often too complicated to be fully understood. A third and less developed method is by chemotaxis, gravitaxis, or phototaxis,[29−38] where a micromotor (especially those powered by

Received: March 17, 2019
Accepted: July 2, 2019
Published: July 2, 2019

DOI: 10.1021/acsnano.9b02100
ACS Nano XXXX, XXX, XXX−XXX

phoretic mechanisms) move up or down a gradient of chemicals, gravity, or light. However, our current understanding of how micromotors interact with a gradient is still rather poor and not without debate.

Besides taxis, living systems often rely on self-assembled tracks that enable well-controlled transport at nano- and microscales. Prominent biological examples include intracellular microtubules and actin, along which biomotors such as kinesin and myosin walk and transport cargos. Synthetic microtracks for guiding micromotors are, on the other hand, rare. One notable example in 2007 demonstrated magnetic bacteria and magnetic microrod swimmers moved on the striped magnetic domains of a magnetic garnet film.[39] Yet this guiding strategy suffers from the fact that the geometries and locations of magnetic domains are entirely random and that swimmers need to be magnetic. A few years later, Yoshizumi et al. pioneered another strategy to guide the motion of bimetallic Janus micromotors in 1D and 2D by exploiting AC electrokinetics on coplanar electrodes.[40] Upon applying AC electric fields of kHz frequencies, Au−Pt Janus microspheres were shown to move along electrodes, and their 2D trajectories can even be controlled by patterning electrodes on both the bottom and the top surfaces. This work mostly focused on the trajectory control of one particular type of chemically driven micromotors, and one naturally wonders whether this electrode-based guiding strategy can be made more generic and useful and what collective behaviors of micromotors could emerge.

Inspired by the idea of micromotors walking on one-dimensional tracks, as well as the questions raised above, we here report a generic strategy to confine, propel, and collect metallodielectric Janus microspheres (e.g., SiO_2−Ti) by using a simple interdigitated microelectrode design under an alternating electric field (AC field). Interdigitated microelectrodes (IDEs) are known to exhibit a rich variety of AC electrokinetics[41,42] and are popular in the applications of detection and separation of biological samples[43,44] as well as biochemical and electrochemical sensing.[45,46] IDEs have even proven useful in the elucidation of propulsion mechanisms of bimetallic microrods.[47] In the current study, particles are electrokinetically propelled via induced charge electrophoresis (ICEP) along the electrode center toward either end of the electrode and are confined by electroosmotic trapping originated at the electrode edges. No additional fuel is needed. The propulsion and confinement of a Janus particle, as well as their interactions both within a pair and within a dense population, are described and explained. In addition, particles turn at the closed end of an electrode but slow down and become collected at electrode openings, whereby a simple modification of the electrode configuration causes a dense populations of Janus particles to form labyrinth patterns made of serpentine chains. This study offers a rather generic, electrode-based strategy for controlling micromotors along a 1D track in a configurable, switchable, and contactless fashion. Importantly, their 1D transport and collection into large, dense piles are potentially useful for fundamental studies of active matters, as well as for sensing, sorting, and delivery applications. These aspects, along with other comments on our findings, are detailed in the Discussion sections at the end.

RESULTS

Single Particle Dynamics. We first describe and explain the dynamics of a single metallodielectric Janus particle on microelectrodes, illustrated in the Supporting Information (SI), Video S1. These microelectrodes are configured in an interdigitated manner, thus upon connecting to a power source of alternating currents each finger electrode is neighbored by two electrodes carrying the opposite electric potential. The top and side views of an experimental chamber containing interdigitated gold microelectrodes on a glass substrate is illustrated in Figure 1a, and an optical micrograph of a typical

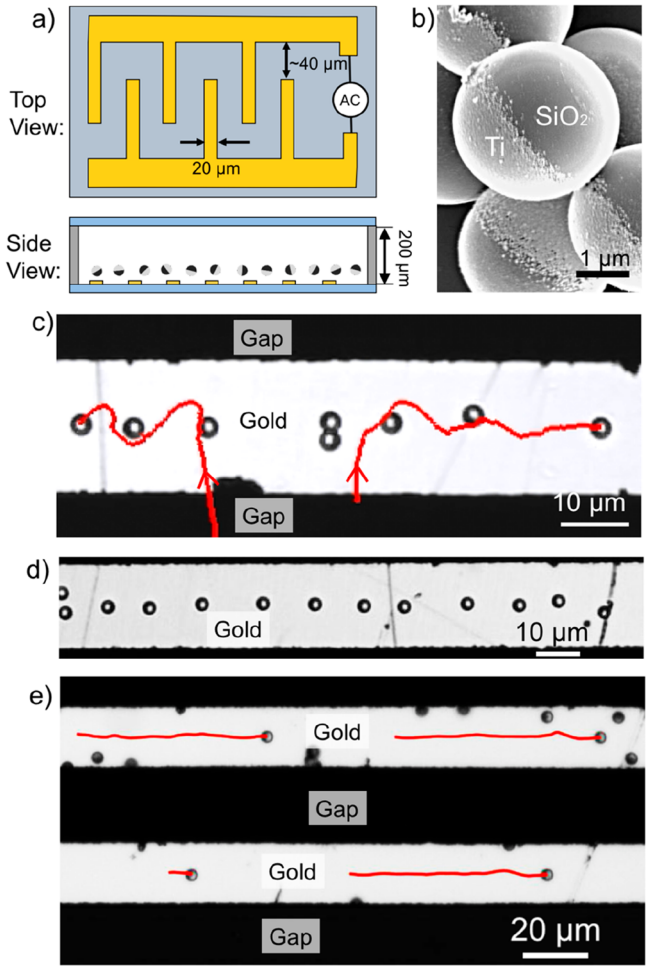

Figure 1. SiO_2−Ti Janus particles and interdigitated microelectrodes (IDEs). (a) Schematics of the top and side view of a chip containing interdigitated gold microelectrodes on a glass substrate. Janus particles sedimented near the electrode surface. (b) Scanning electron micrograph of SiO_2−Ti Janus particles fabricated by evaporating a thin layer of Ti on SiO_2 microspheres. (c) Optical micrograph of a few SiO_2−Ti Janus particles on a gold electrode (bright colored) 3 s after the electric field was switched on. The trajectories of two Janus particles migrating from the gap (dark) to the electrode center are shown in red. (d) Janus particles confined in a line on an electrode under an AC electric field. (e) Trajectories of four Janus particles being propelled for 4 s along the electrode centers.

interdigitated microelectrodes (IDEs) can be found in SI, Figure S7a. Janus SiO_2−Ti particles (Figure 1b) were used in our experiment and were fabricated by evaporating a thin layer of Ti on the surface of SiO_2 microspheres of 3 μm in diameter. Details on the configurations of IDEs and fabrication of Janus particles can be found in the Methods section at the end of the manuscript. Note that all IDEs used in this study, with the

DOI: 10.1021/acsnano.9b02100
ACS Nano XXXX, XXX, XXX−XXX

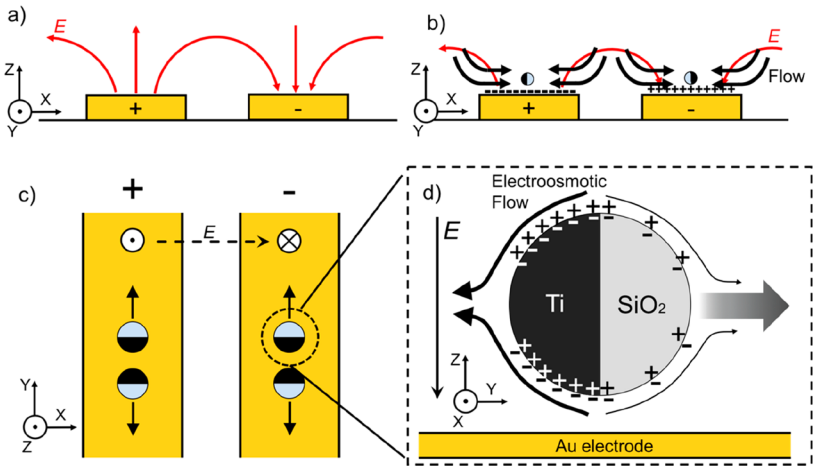

Figure 2. Electrokinetics responsible for the 1D confinement and transport of metallodielectric Janus particles on IDEs. (a) Schematic of the distribution of electric fields (red arrows) on and near a pair of electrodes with opposite electric potential. (b) Tangential components of the electric fields couple with the charged double layer of an electrode, inducing electroosmotic flows (black arrows) that sweep Janus particles toward the electrode center. (c) Top view of the direction and orientation of Janus particles moving on electrodes. (d) Schematic of a SiO_2−Ti particle undergoing induced charge electrophoresis (IECP). See the main text and ref 58 for an expanded discussion of this propulsion mechanism. Although only half a cycle of an AC field is presented in all figures, particle dynamics do not change over the other half cycle.

exception of perhaps those in SI, Figure S7b,c, are commercially available in various dimensions and from various vendors, minimizing the technical hurdle for using this technique.

Upon being transferred into the observation chamber, and in the absence of an electric field, SiO_2−Ti particles quickly sedimented to the bottom of the chamber and covered the entire chip and underwent Brownian motion typical for colloids of such scale. When an AC voltage was applied to IDE, however, SiO_2−Ti particles in the gaps between gold microelectrodes immediately migrated to the center of the gold electrodes (bright regions in all optical micrographs, Figure 1c) and formed a line (Figure 1d), where they spontaneously adjusted orientation so the interface separating Ti and SiO_2 hemispheres were aligned perpendicular to the electrode surface. After migration and reorientation, SiO_2−Ti particles moved along the electrode centerline toward either end of the electrode with their SiO_2 hemispheres pointing forward (Figure 1e), as if being transported on an invisible one-dimensional (1D) track. Note that the accumulation of Janus particles on the surface of gold electrodes, rather than within gaps, is somewhat surprising, as numerous previous studies with coplanar electrodes have mostly focused on the transport and assembly of colloids (Janus or not) within the gap between two electrodes.[48−51]

The confinement and 1D transport of SiO_2−Ti particles on IDEs described above can be qualitatively understood in the following way. AC electric fields applied on IDEs produced electric field lines that pointed outward and inward on neighboring electrodes, respectively (illustrated in Figure 2a), as confirmed by numerical simulations (SI, Figure S4). The electric field lines can be separated into horizontal and vertical components. The horizontal electric field lines exerted an electrical body force on the charged double layer of the electrode surface, inducing an electroosmotic flow (Figure 2b) that pointed from the gaps toward an electrode and converged at its center. Its profile and magnitude is quantified in a later section (see Figure 5). Such an electroosmotic flow on alternating electrodes has been previously discovered in coplanar microelectrodes with similar configurations to ours[40,52,53] and are known to reach tens of micrometers into a microelectrode along its surface.[54] Consequently, Janus particles scattered all over the bottom of an IDE chip were convected by this electroosmotic flow toward the center of the electrode surfaces (Figure 1d), where they were confined, in a way similar to how optical or acoustic tweezers trap colloidal particles. When driven at sufficiently large voltages and low frequencies, electroosmotic flows converge at the center of an electrode, and Janus particles are therefore carried upward and away from the electrode surface (SI, Video S2). This upward convection is carefully minimized in the following studies. Importantly, this induced electroosmosis was maintained inward at all times, despite that alternating AC fields were applied, because the signs of the charges on an electrode surface changed concurrently with the alternating electric fields.

The vertical component of the electric field pointing in and out of electrodes, on the other hand, reorients a Janus particle to align its equator perpendicular to the electrode surface (Figure 2c.). This is because metallodielectric Janus particles, such as SiO_2−Ti, are electrically polarizable and prefer to align their equators parallel to the electric fields to maximize electrical polarization and therefore minimizing energy. Such a reorientation of metallodielectric Janus particles along an electric field line is a common feature in the literature and can give rise to in-plane and out-of-plane dipolar interactions that enable particle assembly into ordered structures.[55] We note, however, that assembly of Janus particles, either parallel or vertical to the electrode plane, was not observed in our experiments at driving frequencies between ∼1 and 100 kHz.

Confined to the electrode center and aligned with its equator vertical to the electrode surface, a SiO_2−Ti Janus particle moved along the centerline of an electrode by induced charge electrophoresis (ICEP) (Figure 2d).[56−58] To briefly introduce this mechanism, the Ti hemisphere, being metal, polarizes much more strongly than SiO_2 hemispheres in an electric field, and more charges are induced on the surface of Ti. The two hemispheres therefore attract different amounts of counterions from the solution in the electrical double layer. Under an electric field, the charged double layers move by

DOI: 10.1021/acsnano.9b02100
ACS Nano XXXX, XXX, XXX−XXX

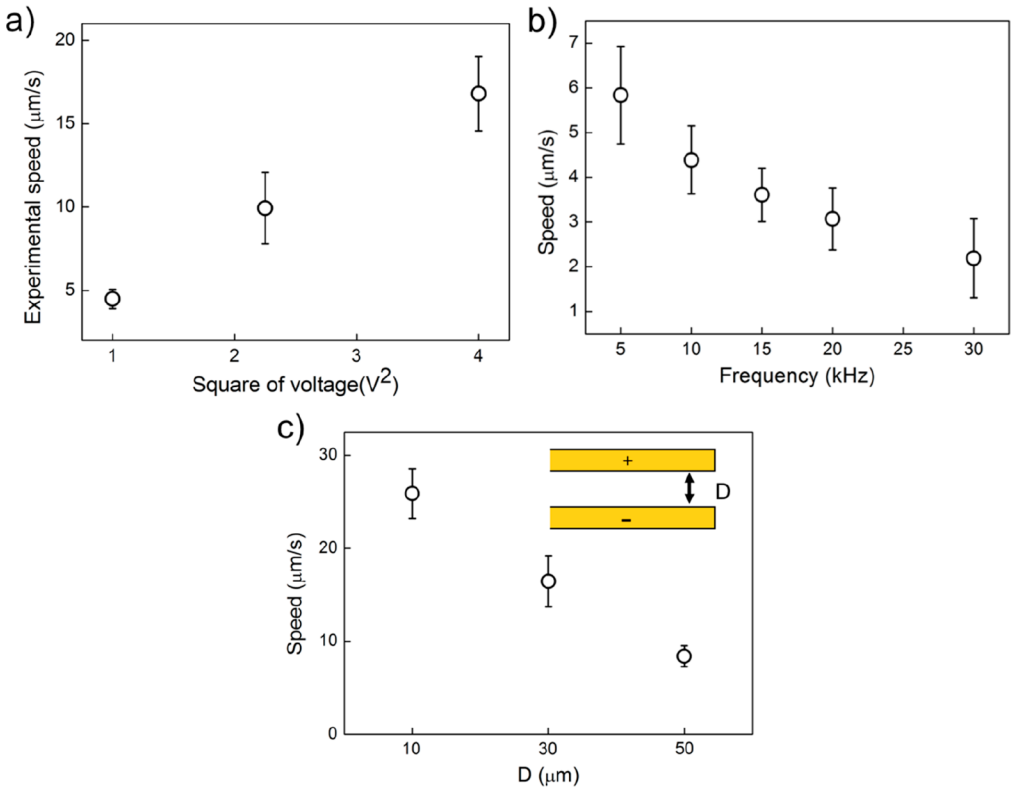

Figure 3. Tuning the speed of SiO_2−Ti Janus particles. (a) Speeds of Janus particles under different driving voltages (peak to peak). Experiments were carried out at 10 kHz with a gap size of 30 μm. (b) Speeds of Janus particles at different driving frequencies. Experiments were carried out at 1 V_{p-p} with a gap size of 30 μm. (c) Speeds of Janus particles using IDEs of different gap widths. Experiments were carried out at 2 V_{p-p} and 10 kHz.

electroosmosis that is more intense on the Ti side than that on the SiO_2 side. Janus particles therefore move away from their metal hemispheres. Janus particles undergoing ICEP has in recent years been employed as a model active colloidal system to investigate interparticle interactions and collective behaviors,[59] the concept of effective temperature,[59] dynamic assembly,[60] and active steering,[61] to name a few. Although driven by the same mechanisms, Janus particles demonstrated here walk on narrow planar microelectrodes rather than being sandwiched between two pieces of indium−tin oxide (ITO) glass, which is the typical configuration used in most of current literature. In addition, unlike earlier studies carried out with planar electrode configurations where Janus particles moved within the gap between two oppositely charged electrodes,[58] in our experiments, they moved on the surface of IDEs (rather than in the gaps) as a result of strong electroosmotic trapping among tightly spaced microelectrodes. We emphasize that it is such a difference in electrode configuration that leads to unusual observations such as 1D transport, U-turns, and collection at electrode exit. These observations are significantly different from those made in previous studies and will be discussed in more detail in a later section.

Before moving on to controlling motor dynamics and more complicated interparticle interactions, we note an interesting observation that particles were often found to stray from the electrode center while moving forward, only to quickly return to the track. Such a fluctuation in particle direction phenomenologically resemble an under-damped oscillator. To qualitatively understand such oscillations, we suspect that the rotational diffusion of a SiO_2−Ti Janus particle, when coupled with its active propulsion, moves the particle toward one side of the electrode. As the particle deviates from the center, however, it is forced to rotate its body and turn back due to the electroosmotic flow and now move toward the other electrode where it will turn back again by the trap. After a few such oscillations, a Janus particle eventually aligns its hemispheres properly and moves forward linearly, while damping could be due to dissipation by hydrodynamic friction. Because rotational diffusion is inevitable and quite significant under our current experimental conditions, particles hardly move in an absolutely linear trap. This track is therefore considered pseudo-1D. Efforts in minimizing such fluctuations is under way, but increasing or decreasing the driving voltage was ineffective because it changed both the trapping and straying force proportionally.

To summarize the cause of the observed single particle dynamics: the horizontal component of the electric fields on and around an interdigitated microelectrode gives rise to lateral electroosmosis that traps a Janus particle to the center of an electrode, while the vertical electric field component orients a Janus particle and induces ICEP that propels it forward in 1D within the electroosmotic trap.

Tuning the Speed of a Janus Particle on IDEs. The design of interdigitated electrodes not only confines metallodielectric Janus particles in 1D tracks but also enables the tuning of their speeds via varying a number of experimental parameters, particularly the driving voltages, frequency, and gap widths of IDEs (Figure 3). First, it is known that the speed of a Janus particle undergoing ICEP is proportional to the second power of the electric field strength via the following:[58]

DOI: 10.1021/acsnano.9b02100
ACS Nano XXXX, XXX, XXX−XXX

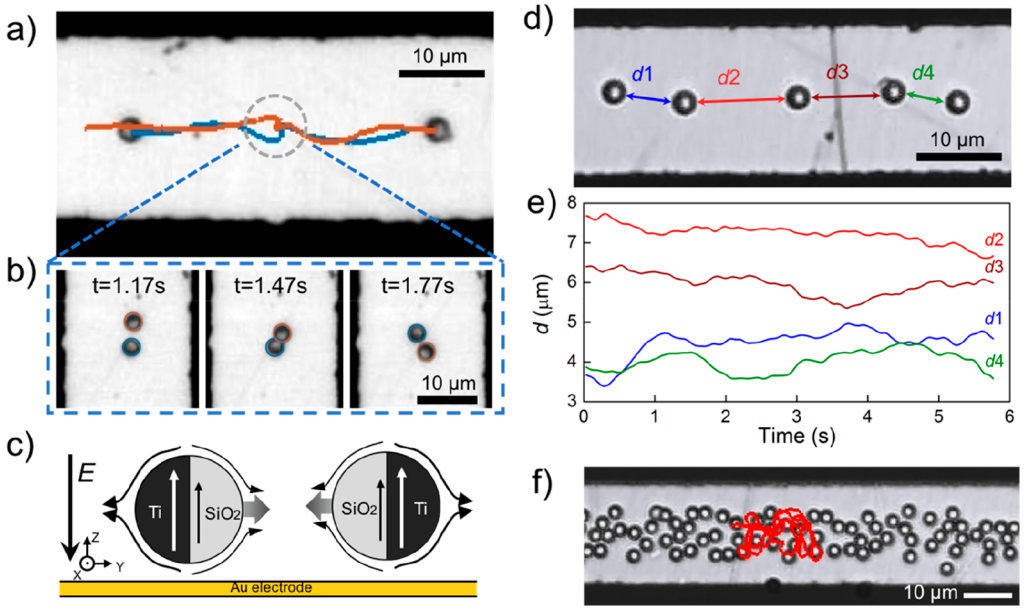

Figure 4. Interactions between SiO_2−Ti Janus particles moving on IDEs. (a) Trajectories of two Janus particles during an encounter (snapshot captured from SI, Video S3). A close-up of the circled part in (a) is shown in (b) with time stamps. (c) Schematic of the two Janus particles in (a) and (b), illustrating their electrical polarizations (arrows on particles) and flow lines (curved arrows around particles). Both the dipolar interactions and hydrodynamic interactions between these two particles are repulsive. (d) Optical micrograph of five Janus particles moving in the same direction (snapshot captured from SI, Video S4). Their interparticle distances are labeled d1 through d4 and are plotted over time in (e). (f) Chaotic trajectory of one Janus particle in a dense, turbulent group (snapshot captured from SI, Video S5).

$$U_{\mathrm{ICEP}} = \frac{9}{64}\frac{\varepsilon R E^2}{\eta(1+\delta)} \quad (1)$$

where ε is the electrical permittivity of the medium, R is the radius of the spherical particle, η is the medium viscosity, E is the electric field strength, and δ is the ratio of the differential capacitance of the compact layer to the diffusion layer (an intrinsic parameter of the electrical double layer that changes over solution ionic strength). Since E scales with the driving voltage when other parameters are fixed, one naturally expects that the speeds of SiO_2−Ti Janus particles on IDEs are proportional to the second power of the driving voltage. This is indeed confirmed in our experiments (Figure 3a).

Figure 3b shows that the average velocity of the particles gradually decreases as the frequency of the electric field was increased from 5 to 30 kHz. No motion was observed at or below 1 kHz, or above 100 kHz, similar to previous reports of ICEP made with coplanar or sandwiched configurations of electrodes.[58,59] A mismatch of time scales is responsible for this frequency window. More specifically, at low driving frequencies (e.g., <1 kHz), the charged double layer on the *electrode* surface could alternate its polarization in sync with the applied electric field, thus effectively screening the electric field outside the double layer. As a result, a Janus particle on an electrode surface was only very weakly polarized and ICEP was consequently weak. Increasing the driving frequency causes the double layer on the electrode surface to not be able to catch up, and Janus particles begin to move under ICEP. However, at much higher driving frequencies (e.g., >100 kHz), the rapidly switching electric field was too fast for ions in the double layer of the *Janus particles* to respond to, and ICEP was therefore shut down. Such an analysis of differences in time scales has been eloquently given in ref 62. Moreover, although previous studies showed that metallodielectric Janus particles reversed their direction when the driving frequency was raised above tens of kHz,[59,61,63,64] this was not observed in our experiments, which raised an interesting point that this reversal could depend on electrode configurations.

Coming back to eq 1, the electric field strength E is also affected by the gap width D between two neighboring electrodes approximately *via* $E = \Delta V/D$, where ΔV is the difference in the electric potential between two neighboring electrodes. Numerical simulations show deviations from this simple estimate near the electrode edges (SI, Figure S5), where the field strength is the highest. Nevertheless, this simple scaling suggests that as the gap width D increases, the electric field strength at the electrode center would decrease proportionally, resulting in a slower Janus particle undergoing ICEP according to eq 1. This is confirmed in our experiments, where particle speeds were measured on IDE electrodes with gap widths of 10, 30, and 50 μm, as shown in Figure 3c. Indeed, electrodes with the smallest gap yielded fastest Janus particles.

Particle−Particle Interactions. Having quantified and explained the single particle dynamics on IDEs, we move on to particle−particle and particle−electrode interactions. A Janus particle moving along the center line of an electrode can move toward either direction. When two particles moving in opposite directions encountered each other, the scenario that occurred most often in our experiments was that the pair moved past each other by slightly reorienting their bodies (Figure 4a,b, and SI, Video S3). Less frequently, one particle in the pair would completely reverse its direction before moving in contact with the opposite particle. In very rare situations, two particles could also collide head-on and stay still for a short period of time before gliding past each other and continuing their separate ways. These observations suggest that between two Janus particles approaching each other from opposite directions there is in-plane repulsion (Figure 4c), which when

DOI: 10.1021/acsnano.9b02100
ACS Nano XXXX, XXX, XXX−XXX

coupled with the rotational diffusion of Janus particles, leads to their reorientation.

The repulsion between two approaching SiO_2−Ti particles could originate from electrical dipolar interactions and hydrodynamic interactions (Figure 4c). More specifically, a previous calculation by Yan et al. (see Figure 2c of ref 59) showed that at a driving frequency around 10 kHz, the typical frequency used in our experiment, both the SiO_2 and Ti hemispheres are electrically polarized in the same direction. As a result, two approaching Janus particles would repel each other via a repulsive dipolar interaction.[55,65] In addition, previous theoretical and experimental studies have found that the flows near a particle undergoing ICEP point outward near its front and rear ends (and inward at the equator), thereby causing a hydrodynamic repulsion between two ICEP particles moving toward each other.[66−69] However, because the electrical polarization is weak for the leading SiO_2 hemisphere of a SiO_2−Ti Janus motor, both the dipolar interaction and hydrodynamic flows between two approaching SiO_2 hemispheres are weak. Two motors were therefore able to briefly collide before they moved past each other rather than repelling each other from far apart as recently demonstrated by two approaching Janus motors with strong magnetic dipolar repulsion.[70]

Unlike those approaching each other, Janus particles moving in the same directions preferred to maintain a certain distance away while moving in a single file. Figure 4d,e demonstrated such a procession of 5 SiO_2−Ti Janus particles moving along the center line of an electrode (SI, Video S4). Although their interparticle distances fluctuated over time, the relative position of all five particles remained largely stable (Figure 4e). One can naively attribute this stable sequence to the fact that all Janus particles were more or less of the same sizes and composition and would therefore move in similar speeds, but additional repulsive interactions could also contribute, such as the dipolar interactions and hydrodynamic interactions discussed earlier.[59] We note that a stable procession of multiple particles could be disrupted by defects along the way, including scratches or particles stuck on the electrode surface or by the end of an electrode, where particles are forced to turn 180° and travel back (SI, Video S6, and discussed in more detail later). Despite these limitations, hydrodynamic trapping of colloidal particles into a 1D chain at an electrode could prove to be a useful technique for the study of single file diffusion,[71−74] especially that of active particles.[75] This will be discussed further in the Discussion section.

As the particle number density is increased, the directional transport of SiO_2−Ti Janus particles along the electrode gave way to chaos (SI, Video S5). One snapshot from SI, Video S5 is given in Figure 4f, and the trajectory of one Janus particle within a dense group is plotted in red, illustrating how it was unable to break free even though its average speeds (and that of its neighbors) remained high. Apart from the crowdedness that hindered the directional transport of Janus particles, they appeared to be actively repelling each other, possibly via dipolar and hydrodynamic interactions discussed earlier that quickly escalated in complexity due to many-body interactions in a strongly confined environment. Because of these interactions and constraints, any one Janus particle of a dense, active group finds it extremely difficult to move far (and is even forced to turn around), and the whole group becomes "active turbulence". Similar turbulence of active particles such as magnetic spinners,[76] bacteria,[77] and cells,[78] have been recently discovered in 2D systems driven far from equilibrium, and such mesoscale turbulence can even be put into useful work.[79] Our system therefore presents a promising playground for studies of active turbulence, and this is discussed further in the Discussion section.

At the Two Ends of Electrodes. So far we have described the dynamics of SiO_2−Ti particles in a quasi-1D confinement defined by the electrode edges on both sides while particles are free to move along the center line of the electrode. What happens when these particles reach the end of an electrode? To begin with, we note that the characteristic configuration of an interdigitated electrode dictates that one end of the finger is a closure (a dead end), while the other end opens to a much bigger gold pad where half of all the fingers are connected to (see Figure 5a for schematics). Therefore, a Janus particle moving along the long axis of an electrode for an extended period of time could very likely reach either end of the electrode.

At the electrode dead end (Figure 5b, SI, Video S6), the particle is forced to make a U-turn and go back along the center line of the electrode. The inward electroosmotic flow along the long axis of the electrode, which shares the same origin as the flow that confines particles from electrode sides, is most likely responsible for the reversal of an incoming Janus particle when coupled to its rotational diffusion. Other sources of repulsion, such as dielectrophoresis,[48] is likely too small to contribute because the particle reversed ∼20 μm away from the electrode dead end.

To further examine the effect of this electroosmotic flow on the reversal of a Janus particle, we measured the instantaneous speeds (U) of 10 micromotors before (U_{before}) and after (U_{after}) they made U-turns (Figure 5c). If we consider U as the combined result of electroosmotic drag forces that pushes a particle away from the electrode end (F_{EO}) and ICEP propulsive forces which always move the particle away from its metal cap (F_{ICEP}), then we have $U_{before} = U_{ICEP} - U_{EO}$ and $U_{after} = U_{ICEP} + U_{EO}$ (all speeds are in absolute values). Simple math would then separate the contributions of these two forces, which are plotted in Figure 5d. Results show that a Janus micromotor approaching the electrode dead end is subjected to a vertical electric field that increases its strength first but decays near the end (thus a similar change in U_{ICEP}). In addition, the electroosmotic flow along the long axis of an electrode is the strongest ∼20 μm inside the electrode, a profile in qualitative agreement with both literature reports and our measurements with tracer microspheres (see SI, Figure S6) in similar electrode configurations.

A Janus particle moving near the open end of an electrode, on the other hand, gradually slowed down as it neared the exit (SI, Video S7). The trajectory of one decelerating Janus particle is presented in Figure 5e, and the instantaneous speeds of four consecutive Janus particles as they exited the same electrode are plotted in Figure 5f (data acquired from SI, Video S7). To understand the observed change of particle speed, we examined via numerical simulation the changes in electric field strength along the center line of an electrode. Simulation results revealed that the second power of the field strength at the exit of an electrode is only roughly 1/10 of that deep in the electrode (Figure 5f, solid line), which matches well with the change in particle speeds measured experimentally (Figure 5f, empty dots). The physical reason for the decline of the electric field is as follows: the configuration of IDEs is such that each electrode finger is ∼40 μm shorter than

DOI: 10.1021/acsnano.9b02100
ACS Nano XXXX, XXX, XXX−XXX

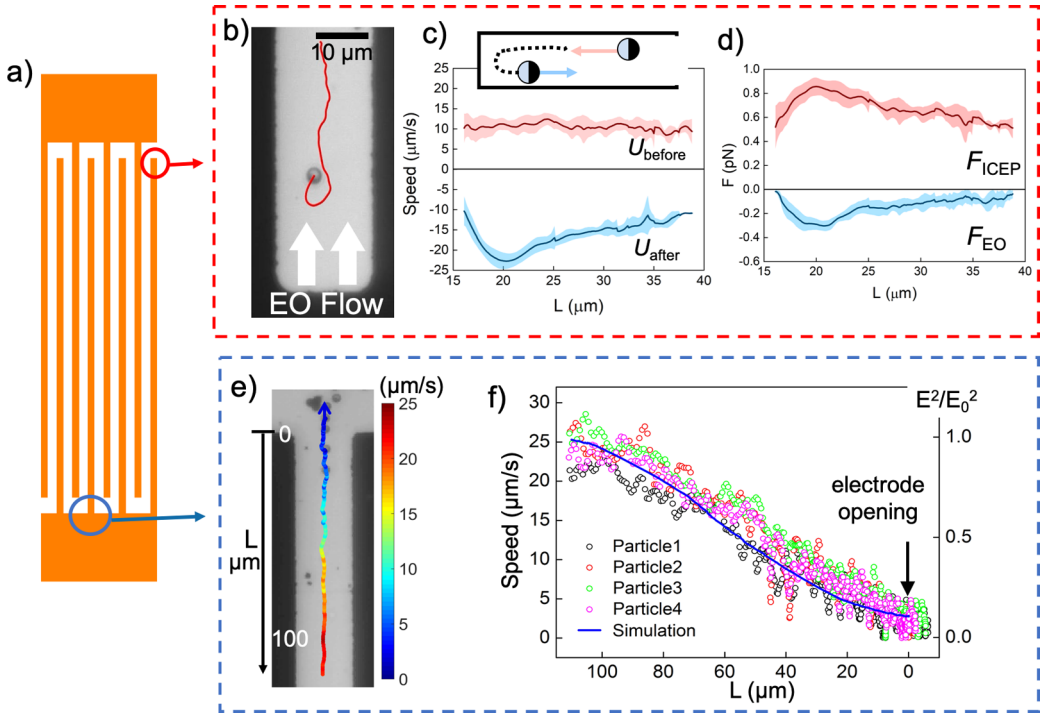

Figure 5. SiO_2−Ti Janus particles moving close to electrode ends. (a) Schematic of the configuration of IDEs, showing closed ends (circled red) and open ends (blue). (b) Optical micrograph of a Janus particle turning around near the closed end of an electrode, with white arrows indicating the electroosmotic flows and a red line indicating the particle trajectory during 3.6 s. (c) Instantons speeds of 10 micromotors before (top, red) and after (bottom, blue) making U-turns. (d) Calculated ICEP propulsive forces (F_{ICEP}, top, red) and electroosmotic drag forces (F_{EO}, bottom, blue) from (c). (e) Optical micrograph showing the trajectory (instantaneous speeds are color coded) of a Janus particle moving toward the open end of an electrode. (f) Instantaneous speeds of four consecutive Janus particles moving toward the electrode opening (scattered data points). *L* is defined as the distance from the opening into an electrode. Simulation results (solid line) confirm the change of electric field strength along the long axis of an electrode toward its opening.

the separation between two electrode pads (Figure 1a). This means that the two closest neighboring electrodes of −V will have closed up long before the middle electrode of +V opens to the large pad. As a result, the gap *D* between electrodes widens as a Janus particle moves close to the electrode opening, and the electric field it experiences decreases in proportion.

A natural consequence of the above two scenarios, turning around at the dead end and slowing down at the open end of an electrode, is that Janus particles that were initially uniformly scattered on the entire chip surface would eventually be collected at the electrode openings. Figure 6a and SI, Video S8 demonstrates this process, where after 20 s a large number of particles had accumulated at the openings of all the fingers (although Figure 6a only shows one side of the whole IDE chip, the same is observed on the other side). The pile of particles was fan-shaped, likely because of the electroosmotic flow pointing from gaps into electrodes (Figure 6a, white arrows in the last panel).

Although Janus particles on the large gold pad at the electrode exit show little activity beyond Brownian motion, they can be easily activated by slightly modifying the electrode configuration. An example is given in Figure 6b, where the inert glass top cover of the experiment chamber in Figure 1a is replaced with a conductive ITO glass (coating facing down). Upon electrically connecting this ITO layer to one set of the finger electrodes, the expelled Janus particles on the large pad now experiences an additional vertical AC electric field generated between the bottom gold pad and the top ITO. As a result, they move and interact in the same way as in a typical ITO sandwich configuration (SI, Video S9). For example, Figure 6c shows the formation of SiO_2−Ti Janus particles of labyrinth patterns made of serpentine chains, similar to a previous report carried out with a ITO sandwich setup.[64]

DISCUSSION

The core idea of this manuscript is to introduce interdigitated microelectrodes (IDEs) as a useful platform for the study of active matters (micromotors in particular), where electroosmotic trapping confines particles in 1D tracks and ICEP propels them along the track. Following the descriptions of the rich dynamics of Janus metallodielectric particles shuttling on these electrodes and their interactions, we in this section discuss the following three aspects that suggest practical usefulness of this strategy: (1) the difference and advantages of electroosmotic trapping compared to other trapping techniques, (2) the usefulness of confined propulsion of Janus particles on IDEs in the study of active matters, and (3) the generality of this technique in terms of particle selections and electrode designs.

First, the electroosmotic trapping demonstrated with these IDEs are different from other major strategies that confine micromotors. Previously, physical boundaries such as tight channels,[80,81] trenches,[82,83] edges,[84] pillars,[85] and heart-shaped structures[86] were fabricated by lithography and were able to geometrically limit and guide the transport of micromotors moving nearby. However, physical boundaries also introduce a complicated interplay of electrostatics, electrokinetics, hydro-

DOI: 10.1021/acsnano.9b02100
ACS Nano XXXX, XXX, XXX−XXX

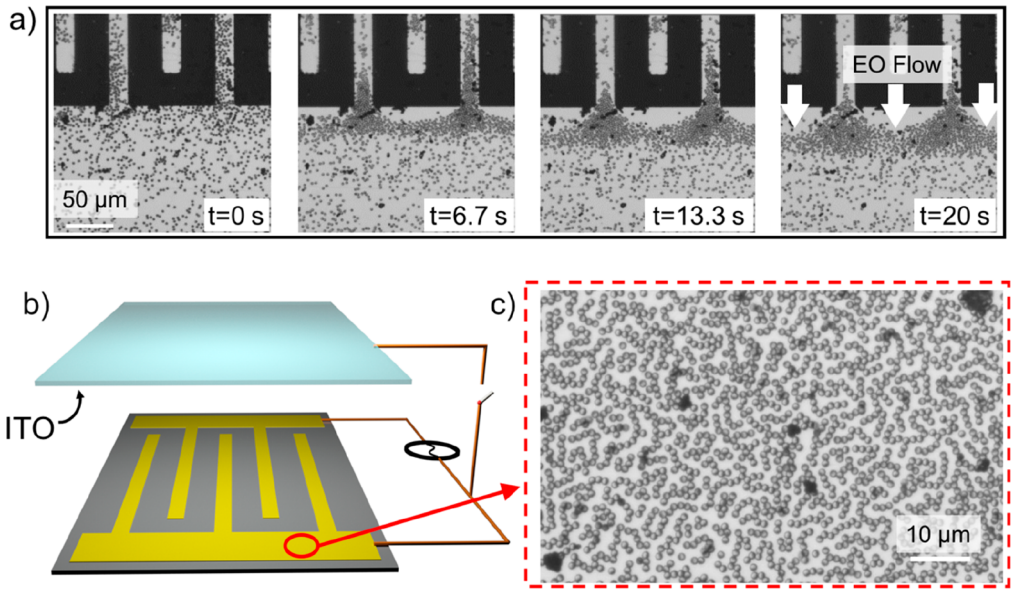

Figure 6. Accumulation of Janus particles at the electrode openings. (a) Time elapsed optical micrographs over 20 s at the openings of the electrodes, with white arrows indicating the electroosmotic flows. (b) Modified electrode configuration. The top cover is replaced with an ITO-coated coverslip, which is electrically connected to the bottom electrode with a switch. (c) Upon turning on the switch from (b), a vertical electric field between the top and bottom electrodes activate the accumulated piles of Janus particles in (a), forming labyrinth patterns made of serpentine chains.

dynamics, and steric effects between a microswimmer and a surface with which it is in close contact. This feature is not only poorly understood but could also be mechanism-dependent so that it only applies to certain types of micromotors. The other major limitation is the lack of an on−off mechanism to enable and disable the confinement as needed. Once a microswimmer suspension is added to these physical structures, there is very little control over when the particles become confined and how (or whether) they can be released.

In contrast, electroosmotic trapping offers an alternative strategy that addresses both issues, by being easily turned on and off and by being contactless. (Note that although our experiments involve a charged boundary at the bottom, it does not confine particles in the sense that is discussed here.) Although optical or acoustic trapping also exhibit both features,[87] electroosmotic trapping compares favorably in that it applies to a wider range of particles, including metallodielectric Janus particles that would spontaneously spin in either optical or acoustic traps.[88,89] The much less complicated experimental setup of electroosmotic trapping techniques is another advantage.

There are certainly limitations to be noted too. For example, the trapping force exerted on a Janus particle in our experiment is on the order of pN, smaller than intense trapping offered by optical or acoustic trapping. Motors are therefore only loosely confined in a somewhat flexible track, especially if the driving voltage (therefore electroosmotic flow magnitude) is small. The trapping potential is also less well-defined, with possible defects and inhomogeneity as a result of electrode fabrication. In addition, due to fluid continuity, a trapped particle is often in an unstable state, easy to be convected upward or downward by converging flows, or trapped in a vortex. Finally, even though a hydrodynamic trap is contactless and on/off-switchable, features that are missing from physical constraints, both trapping techniques require microfabrication and are therefore more or less fixed/static. Optical or acoustic traps are on the other hand dynamic and promise spatiotemporal manipulation. It is perhaps only fair to compare these trapping techniques on a scenario-specific base.

Given its features and limitations, we envision the fast and on-demand collection and enrichment of active particles at specific locations demonstrated in this study could prove particularly useful in a few scenarios. First, by mixing Janus SiO_2−Ti particles with bare SiO_2 microspheres, we see that Janus particles move along the electrode center and plough through clusters of inactive SiO_2 spheres (SI, Video S10). With proper surface chemistry and selection of particles, this could be useful for biosensing and cell/bacteria separation based on specific surface−surface interactions.[90,91] In addition, due to a difference in activity, Janus particles and non-Janus particles can be sorted by collecting Janus particles at the electrode exits. Second, the collection of a dense population of particles at the electrode exits could serve as a useful technique for the study of collective behaviors of active matter in a dense population,[92−98] such as jamming, swarming, phase separation, *etc.* Unlike conventional techniques for these studies that involve concentrated particle suspensions, enriching particles with IDEs requires much fewer samples, a great benefit for samples that do not come in large quantities (such as cells). Third, the current setup enables interesting possibilities for studying single file diffusion of active particles and their collective behaviors in a strongly confined and driven system. Single file diffusion seen in Figure 4d and active turbulence seen in Figure 4f may very well be the two ends of a spectrum of rich dynamics. For example, a previous study of the emergent band of Quincke rollers moving along a racetrack[99] suggests that confining a dense group of interacting, motile active particles does NOT necessarily lead to turbulence, in contrast to our observations. There seems to be a phase transition from turbulence to order (or vice versa) among densely populated active particles that is regulated by the degree of confinement and/or the nature and strength of

DOI: 10.1021/acsnano.9b02100
ACS Nano XXXX, XXX, XXX−XXX

interparticle interactions. Our current setup, upon modification, could prove useful for probing this very interesting question with far-reaching impact.

Finally, we briefly comment on the generality of the observed confinement and propulsion of Janus particles on IDEs. The propulsion of particles is activated by an asymmetric electrical polarization of a Janus particle under AC electric fields, and this naturally applies to other metallodielectric particles beyond SiO_2−Ti demonstrated here. Pt coated polystyrene microspheres, for example, exhibited qualitatively the same behaviors (results not shown). It is perhaps important to note that this propulsion mechanism is somewhat insensitive to the surface functionalization (e.g., gold surface functionalized with −SH that enables streptavidin−biotin binding), facilitating biological applications. Confinement, on the other hand, emerges from the electroosmotic flows pointing inward the electrodes from the gaps, and this effect can be easily reproduced by microelectrodes of configurations beyond simple parallel electrodes. For example, we have fabricated via photolithography microelectrodes that are aligned not parallel but with a small offset angle (SI, Figure S7b), as well as those curling into spirals (SI, Figure S7c), and observed qualitatively the same confinement and propulsion of Janus particles on these electrodes. More complicated designs could in principle enable the directional transport of active particles along tracks of arbitrary shapes (such as mazes), with controlled left and right turns, toward a specific target. In summary, the great variety in Janus particle selections, in functionalization on either hemisphere, and in microelectrode designs could potentially enable a wide range of applications.

CONCLUSIONS

By combining ICEP propulsion of Janus particles and electroosmotic trapping, we demonstrate a strategy to propel, confine, and collect metallodielectric Janus particles on interdigitated microelectrodes under AC electric fields. Notably, the horizontal component of the electric field induces lateral electroosmotic flows that work as a hydrodynamic trap to confine Janus particles at the electrode centers, while the vertical component of the electric field aligns and propels the particle via ICEP. Interesting observations were also made such as single file diffusion, particle pairwise interactions and active turbulence, turning at electrodes, and collection at the electrode exits, all qualitatively explained by dipolar and hydrodynamic interactions.

Looking forward, this strategy, although primitive and limited at its current stage, could be further developed into functional, tunable tracks that steer synthetic microrobots, as well as a contactless technique to manipulate the organization of active matters, useful for the study of their collective behaviors, single file diffusion, and active turbulence. Limitations with the current demonstration are detailed in the Discussion section. A distinct advantage of microelectrodes is in its tunability, both in the design of its structures and dimensions via lithography and in controlling experimental parameters such as driving voltages and frequencies. Furthermore, the strategy presented here can be extended to other electrode designs and other types of Janus particle.

METHODS

Experimental Setup. Chips containing interdigital microelectrodes used in our experiments were purchased from NanoSPR LLC (Chicago, USA). According to the manufacturer, IDEs were fabricated by evaporating 150 nm of gold on glass substrates, which formed finger electrodes of 20 μm width and separated by regular gaps (three different chips with gap width of 10, 30, and 50 μm were used in our experiments). An observation chamber was made by placing carefully over the IDEs a silicone spacer of 200 μm in thickness with a hole of 5 mm in diameter (Grace Biolabs). Microparticle suspension was added into the chamber by micropipette, and the chamber was sealed from the top by a precleaned glass coverslip. The two sets of finger electrodes of an IDE were connected to a function generator (Agilent33210A) that output alternating signals (square waves) so that neighboring electrodes always carried opposite electrical potential. For example, half of all electrodes carried 1 V while the other half −1 V when 2 V_{p-p} was applied. In a typical experiment, signals of a few volts (peak to peak) operating at a few kHz were applied, although other parameters had been examined and are reported in the main text. Particle motion was recorded by a CMOS camera (Point Gray, Grasshopper 3) mounted on an Olympus BX51 M upright microscope. Reflective microscopy was used, and gold electrodes were therefore bright in color. Particle coordinates were tracked by homemade MATLAB codes, which enabled plotting its trajectories and calculating its instantaneous speeds. A schematic of the experimental setup can be found in SI, Figure S1.

Fabrication of SiO_2−Ti Janus Particles. A monolayer of SiO_2 (3 μm in diameter) was first prepared by a drop-casting method. SiO_2 microspheres was first suspended in ethanol (20 μL) and dispersed by ultrasound. The suspension was drop-casted on a piece of glass slide pretreated by Piranha solution (a mixture of concentrated H_2SO_4 with 30% H_2O_2 in 3:1 volume ratio. Caution! Extremely corrosive!). A thin film of 50 nm Ti was then deposited on the top of the dried SiO_2 monolayer via electron beam evaporation. SiO_2−Ti Janus particles were then collected by sonication and resuspended in deionized water. An SEM image of the fabricated SiO_2−Ti Janus particles is shown in Figure 1b.

Simulations. Our 3D numerical model was implemented with COMSOL Multiphysics package (version 5.2a). IDEs of proper dimensions were sandwiched between bodies of water and glass. Positive and negative electrical potentials were set on alternating electrodes and steady-state solutions of the electric potential and electric fields in the whole domain were calculated. The electrostatic module in COMSOL was used. Details of the simulation, including geometry, boundary conditions, and other parameters, can be found in the Supporting Information.

ASSOCIATED CONTENT

Supporting Information

The Supporting Information is available free of charge on the ACS Publications website at DOI: 10.1021/acsnano.9b02100.

Experimental setup, simulation details, experiments to quantify electroosmotic flow profiles, electrodes of other geometries, detailed descriptions of supporting videos (PDF)

Single particle dynamics of SiO_2−Ti Janus particles on interdigitated microelectrodes (AVI)

Janus particles are convected upward at the center of an electrode by the converging electroosmotic flow coming from the sides (AVI)

Two SiO_2−Ti particles moving in opposite directions encounter and separate (AVI)

Janus particles moving in the same direction in a single file (AVI)

A chaotic group of Janus particles (AVI)

A Janus particle making U-turns at the closure of a finger electrode (located at the bottom of the video) (AVI)

Janus particle slowing down at the open end of an electrode (AVI)

DOI: 10.1021/acsnano.9b02100
ACS Nano XXXX, XXX, XXX−XXX

Accumulation of a large number of particles at the openings of finger electrodes (AVI)

Accumulated Janus particles on the large gold pad can be activated by switching on the vertical electric field (AVI)

An active Janus micromotor ploughs through inert SiO_2 microspheres accumulated at the electrode center (AVI)

AUTHOR INFORMATION

Corresponding Author

*E-mail: weiwangsz@hit.edu.cn.

ORCID

Wei Wang: 0000-0003-4163-3173

Author Contributions

§L.Z. and Z.X. contributed equally.

Notes

The authors declare no competing financial interest.

ACKNOWLEDGMENTS

We are deeply grateful for the helpful discussions with Prof. Steve Granick from IBS CSLM and Prof. Ning Wu from the Colorado School of Mines. We are also very thankful for the help with numerical simulations from Drs. Jie Zhang and Yaroslav I. Sobolev and for the help with microscope setup from Jintae Park, all affiliated with IBS CSLM. This work was supported by Science Technology and Innovation Program of Shenzhen (JCYJ20170307150031119), the National Natural Science Foundation of China (11774075 and 11402069), Natural Science Foundation of Guangdong Province (no. 2017B030306005), and the taxpayers of South Korea through the Institute for Basic Science, project code IBS-R020-D1.

REFERENCES

(1) Chen, X.; Zhou, C.; Wang, W., Colloidal Motors 101: A Beginner's Guide to Colloidal Motor Research. *Chem.—Asian J.* **2019**, DOI: 10.1002/asia.201900377

(2) Wang, J. *Nanomachines: Fundamentals and Applications*; John Wiley & Sons: Hoboken, NJ, 2013.

(3) Wong, F.; Dey, K. K.; Sen, A. Synthetic Micro/Nanomotors and Pumps: Fabrication and Applications. *Annu. Rev. Mater. Res.* **2016**, *46*, 407−432.

(4) Mallouk, T. E.; Sen, A. Powering Nanorobots. *Sci. Am.* **2009**, *300*, 72−77.

(5) Katuri, J.; Ma, X.; Stanton, M. M.; Sánchez, S. Designing Micro- and Nanoswimmers for Specific Applications. *Acc. Chem. Res.* **2017**, *50*, 2−11.

(6) Kim, K.; Guo, J.; Liang, Z.; Zhu, F.; Fan, D. Man-Made Rotary Nanomotors: A Review of Recent Developments. *Nanoscale* **2016**, *8*, 10471−10490.

(7) Yadav, V.; Duan, W.; Butler, P. J.; Sen, A. Anatomy of Nanoscale Propulsion. *Annu. Rev. Biophys.* **2015**, *44*, 77−100.

(8) Colberg, P. H.; Reigh, S. Y.; Robertson, B.; Kapral, R. Chemistry in Motion: Tiny Synthetic Motors. *Acc. Chem. Res.* **2014**, *47*, 3504−3511.

(9) Nain, S.; Sharma, N. Propulsion of an Artificial Nanoswimmer: A Comprehensive Review. *Front. Life Sci.* **2015**, *8*, 2−17.

(10) Pan, Q.; He, Y. Recent Advances in Self-Propelled Particles. *Sci. China: Chem.* **2017**, *60*, 1293−1304.

(11) Kim, K.; Guo, J.; Xu, X.; Fan, D. L. Recent Progress on Man-Made Inorganic Nanomachines. *Small* **2015**, *11*, 4037−4057.

(12) Ebbens, S. J. Active Colloids: Progress and Challenges towards Realising Autonomous Applications. *Curr. Opin. Colloid Interface Sci.* **2016**, *21*, 14−23.

(13) Lauga, E.; Powers, T. R. The Hydrodynamics of Swimming Microorganisms. *Rep. Prog. Phys.* **2009**, *72*, 096601.

(14) Li, J.; Esteban-Fernández de Ávila, B.; Gao, W.; Zhang, L.; Wang, J. Micro/Nanorobots for Biomedicine: Delivery, Surgery, Sensing, and Detoxification. *Sci. Robot* **2017**, *2*, No. eaam6431.

(15) Yeomans, J. M. Active Matter: Playful Topology. *Nat. Mater.* **2014**, *13*, 1004−1005.

(16) Marchetti, M. C.; Joanny, J.-F.; Ramaswamy, S.; Liverpool, T. B.; Prost, J.; Rao, M.; Simha, R. A. Hydrodynamics of Soft Active Matter. *Rev. Mod. Phys.* **2013**, *85*, 1143.

(17) Sanchez, T.; Chen, D. T.; DeCamp, S. J.; Heymann, M.; Dogic, Z. Spontaneous Motion in Hierarchically Assembled Active Matter. *Nature* **2012**, *491*, 431−434.

(18) Tu, Y.; Peng, F.; Wilson, D. A. Motion Manipulation of Micro- and Nanomotors. *Adv. Mater.* **2017**, *29*, 1701970.

(19) Teo, W. Z.; Pumera, M. Motion Control of Micro-/Nanomotors. *Chem. - Eur. J.* **2016**, *22*, 14796−14804.

(20) Ebbens, S. J.; Gregory, D. A. Catalytic Janus Colloids: Controlling Trajectories of Chemical Microswimmers. *Acc. Chem. Res.* **2018**, *51*, 1931−1939.

(21) Wang, J.; Manesh, K. M. Motion Control At the Nanoscale. *Small* **2010**, *6*, 338−345.

(22) Chen, X.-Z.; Hoop, M.; Mushtaq, F.; Siringil, E.; Hu, C.; Nelson, B. J.; Pané, S. Recent Developments in Magnetically Driven Micro-and Nanorobots. *Appl. Mater. Today* **2017**, *9*, 37−48.

(23) Peyer, K. E.; Tottori, S.; Qiu, F.; Zhang, L.; Nelson, B. J. Magnetic Helical Micromachines. *Chem. - Eur. J.* **2013**, *19*, 28−38.

(24) Peyer, K. E.; Zhang, L.; Nelson, B. J. Bio-Inspired Magnetic Swimming Microrobots for Biomedical Applications. *Nanoscale* **2013**, *5*, 1259−1272.

(25) Patteson, A. E.; Gopinath, A.; Arratia, P. E. Active Colloids in Complex Fluids. *Curr. Opin. Colloid Interface Sci.* **2016**, *21*, 86−96.

(26) Katuri, J.; Seo, K.; Kim, D.; Sanchez, S. Artificial Micro-Swimmers in Simulated Natural Environments. *Lab Chip* **2016**, *16*, 1101−1105.

(27) Xiao, Z.; Wei, M.; Wang, W. A Review of Micromotors in Confinements: Pores, Channels, Grooves, Steps, Interfaces, Chains and Swimming in the Bulk. *ACS Appl. Mater. Interfaces* **2019**, *11*, 6667−6684.

(28) Bechinger, C.; Di Leonardo, R.; Löwen, H.; Reichhardt, C.; Volpe, G.; Volpe, G. Active Particles in Complex and Crowded Environments. *Rev. Mod. Phys.* **2016**, *88*, 045006.

(29) Liebchen, B.; Löwen, H. Synthetic Chemotaxis and Collective Behavior in Active Matter. *Acc. Chem. Res.* **2018**, *51*, 2982−2990.

(30) Stark, H. Artificial Chemotaxis of Self-Phoretic Active Colloids: Collective Behavior. *Acc. Chem. Res.* **2018**, *51*, 2681−2688.

(31) Agudo-Canalejo, J.; Adeleke-Larodo, T.; Illien, P.; Golestanian, R. Enhanced Diffusion and Chemotaxis at the Nanoscale. *Acc. Chem. Res.* **2018**, *51*, 2365−2372.

(32) You, M.; Chen, C.; Xu, L.; Mou, F.; Guan, J. Intelligent Micro/Nanomotors with Taxis. *Acc. Chem. Res.* **2018**, *51*, 3006−3014.

(33) Zhou, C.; Chen, X.; Han, Z.; Wang, W. Photochemically Excited, Pulsating Janus Colloidal Motors of Tunable Dynamics. *ACS Nano* **2019**, *13*, 4064−4072.

(34) Campbell, A. I.; Ebbens, S. J. Gravitaxis in Spherical Janus Swimming Devices. *Langmuir* **2013**, *29*, 14066−14073.

(35) Singh, D. P.; Uspal, W. E.; Popescu, M. N.; Wilson, L. G.; Fischer, P. Photogravitactic Microswimmers. *Adv. Funct. Mater.* **2018**, *28*, 1706660.

(36) Zhou, C.; Zhang, H.; Tang, J.; Wang, W. Photochemically Powered AgCl Janus Micromotors as a Model System to Understand Ionic Self-Diffusiophoresis. *Langmuir* **2018**, *34*, 3289−3295.

(37) Hong, Y.; Blackman, N. M.; Kopp, N. D.; Sen, A.; Velegol, D. Chemotaxis of Nonbiological Colloidal Rods. *Phys. Rev. Lett.* **2007**, *99*, 178103.

(38) Lagzi, I.; Soh, S.; Wesson, P. J.; Browne, K. P.; Grzybowski, B. A. Maze Solving by Chemotactic Droplets. *J. Am. Chem. Soc.* **2010**, *132*, 1198−1199.

DOI: 10.1021/acsnano.9b02100
ACS Nano XXXX, XXX, XXX−XXX

(39) Dhar, P.; Cao, Y.; Kline, T.; Pal, P.; Swayne, C.; Fischer, T. M.; Miller, B.; Mallouk, T. E.; Sen, A.; Johansen, T. H. Autonomously Moving Local Nanoprobes in Heterogeneous Magnetic Fields. *J. Phys. Chem. C* **2007**, *111*, 3607−3613.
(40) Yoshizumi, Y.; Honegger, T.; Berton, K.; Suzuki, H.; Peyrade, D. Trajectory Control of Self-Propelled Micromotors Using AC Electrokinetics. *Small* **2015**, *11*, 5630−5635.
(41) Park, S.; Beskok, A. Alternating Current Electrokinetic Motion of Colloidal Particles on Interdigitated Microelectrodes. *Anal. Chem.* **2008**, *80*, 2832−2841.
(42) Ramos, A.; Morgan, H.; Green, N. G.; Castellanos, A. AC Electrokinetics: A Review of Forces in Microelectrode Structures. *J. Phys. D: Appl. Phys.* **1998**, *31*, 2338−2353.
(43) Becker, F.; Wang, X.-B.; Huang, Y.; Pethig, R.; Vykoukal, J.; Gascoyne, P. The Removal of Human Leukaemia Cells from Blood Using Interdigitated Microelectrodes. *J. Phys. D: Appl. Phys.* **1994**, *27*, 2659−2662.
(44) Yang, L.; Li, Y.; Erf, G. F. Interdigitated Array Microelectrode-Based Electrochemical Impedance Immunosensor for Detection of Escherichia coli O157: H7. *Anal. Chem.* **2004**, *76*, 1107−1113.
(45) Van Gerwen, P.; Laureyn, W.; Laureys, W.; Huyberechts, G.; Op De Beeck, M.; Baert, K.; Suls, J.; Sansen, W.; Jacobs, P.; Hermans, L.; Mertens, R. Nanoscaled Interdigitated Electrode Arrays for Biochemical Sensors. *Sensors Actuators B: Chem.* **1998**, *49*, 73−80.
(46) Morita, M.; Niwa, O.; Horiuchi, T. Interdigitated Array Microelectrodes as Electrochemical Sensors. *Electrochim. Acta* **1997**, *42*, 3177−3183.
(47) Paxton, W. F.; Baker, P. T.; Kline, T. R.; Wang, Y.; Mallouk, T. E.; Sen, A. Catalytically Induced Electrokinetics for Motors and Micropumps. *J. Am. Chem. Soc.* **2006**, *128*, 14881−14888.
(48) Gangwal, S.; Cayre, O. J.; Velev, O. D. Dielectrophoretic Assembly of Metallodielectric Janus Particles in AC Electric Fields. *Langmuir* **2008**, *24*, 13312−13320.
(49) Lumsdon, S. O.; Kaler, E. W.; Velev, O. D. Two-Dimensional Crystallization of Microspheres by a Coplanar AC Electric Field. *Langmuir* **2004**, *20*, 2108−2116.
(50) Kretschmer, R.; Fritzsche, W. Pearl Chain Formation of Nanoparticles in Microelectrode Gaps by Dielectrophoresis. *Langmuir* **2004**, *20*, 11797−11801.
(51) Hermanson, K. D.; Lumsdon, S. O.; Williams, J. P.; Kaler, E. W.; Velev, O. D. Dielectrophoretic Assembly of Electrically Functional Microwires from Nanoparticle Suspensions. *Science* **2001**, *294*, 1082−1086.
(52) Green, N. G.; Ramos, A.; González, A.; Morgan, H.; Castellanos, A. Fluid Flow Induced by Nonuniform AC Electric Fields in Electrolytes on Microelectrodes. III. Observation of Streamlines and Numerical Simulation. *Phys. Rev. E: Stat. Phys., Plasmas, Fluids, Relat. Interdiscip. Top.* **2002**, *66*, 026305.
(53) Ramos, A.; Morgan, H.; Green, N. G.; Castellanos, A. AC Electric-Field-Induced Fluid Flow in Microelectrodes. *J. Colloid Interface Sci.* **1999**, *217*, 420−422.
(54) Green, N. G.; Ramos, A.; González, A.; Morgan, H.; Castellanos, A. Fluid Flow Induced by Nonuniform AC Electric Fields in Electrolytes on Microelectrodes. I. Experimental Measurements. *Phys. Rev. E: Stat. Phys., Plasmas, Fluids, Relat. Interdiscip. Top.* **2000**, *61*, 4011−4018.
(55) Velev, O. D.; Gangwal, S.; Petsev, D. N. Particle-Localized AC and DC Manipulation and Electrokinetics. *Annu. Rep. Prog. Chem., Sect. C: Phys. Chem.* **2009**, *105*, 213−246.
(56) Bazant, M. Z.; Squires, T. M. Induced-Charge Electrokinetic Phenomena: Theory and Microfluidic Applications. *Phys. Rev. Lett.* **2004**, *92*, 066101.
(57) Ramos, A.; García-Sánchez, P.; Morgan, H. AC Electrokinetics of Conducting Microparticles: A Review. *Curr. Opin. Colloid Interface Sci.* **2016**, *24*, 79−90.
(58) Gangwal, S.; Cayre, O. J.; Bazant, M. Z.; Velev, O. D. Induced-Charge Electrophoresis of Metallodielectric Particles. *Phys. Rev. Lett.* **2008**, *100*, 058302.
(59) Yan, J.; Han, M.; Zhang, J.; Xu, C.; Luijten, E.; Granick, S. Reconfiguring Active Particles by Electrostatic Imbalance. *Nat. Mater.* **2016**, *15*, 1095−1099.
(60) Boymelgreen, A. M.; Balli, T.; Miloh, T.; Yossifon, G. Active Colloids as Mobile Microelectrodes for Unified Label-Free Selective Cargo Transport. *Nat. Commun.* **2018**, *9*, 760.
(61) Mano, T.; Delfau, J.-B.; Iwasawa, J.; Sano, M. Optimal Run-and-Tumble−Based Transportation of a Janus Particle with Active Steering. *Proc. Natl. Acad. Sci. U. S. A.* **2017**, *114*, E2580−E2589.
(62) Squires, T. M.; Bazant, M. Z. Induced-Charge Electro-Osmosis. *J. Fluid Mech.* **1999**, *509*, 217−252.
(63) Boymelgreen, A.; Yossifon, G.; Miloh, T. Propulsion of Active Colloids by Self-Induced Field Gradients. *Langmuir* **2016**, *32*, 9540−9547.
(64) Nishiguchi, D.; Iwasawa, J.; Jiang, H.-R.; Sano, M. Flagellar Dynamics of Chains of Active Janus Particles Fueled by an AC Electric Field. *New J. Phys.* **2018**, *20*, 015002.
(65) Mittal, M.; Lele, P. P.; Kaler, E. W.; Furst, E. M. Polarization and Interactions of Colloidal Particles in AC Electric Fields. *J. Chem. Phys.* **2008**, *129*, 064513.
(66) Nishiguchi, D.; Sano, M. Mesoscopic Turbulence and Local Order in Janus Particles Self-Propelling under an AC Electric Field. *Phys. Rev. E* **2015**, *92*, 052309.
(67) Rose, K. A.; Hoffman, B.; Saintillan, D.; Shaqfeh, E. S. G.; Santiago, J. G. Hydrodynamic Interactions in Metal Rodlike-Particle Suspensions due to Induced Charge Electroosmosis. *Phys. Rev. E* **2009**, *79*, 011402.
(68) Kilic, M. S.; Bazant, M. Z. Induced-Charge Electrophoresis near a Wall. *Electrophoresis* **2011**, *32*, 614−628.
(69) Peng, C.; Lazo, I.; Shiyanovskii, S. V.; Lavrentovich, O. D. Induced-Charge Electro-Osmosis around Metal and Janus Spheres in Water: Patterns of Flow and Breaking Symmetries. *Phys. Rev. E* **2014**, *90*, 051002.
(70) Nourhani, A.; Brown, D.; Pletzer, N.; Gibbs, J. G. Engineering Contactless Particle−Particle Interactions in Active Microswimmers. *Adv. Mater.* **2017**, *29*, 1703910.
(71) Taloni, A.; Flomenbom, O.; Castañeda-Priego, R.; Marchesoni, F. Single File Dynamics in Soft Materials. *Soft Matter* **2017**, *13*, 1096−1106.
(72) Nelissen, K.; Misko, V. R.; Peeters, F. M. Single-File Diffusion of Interacting Particles in a One-Dimensional Channel. *Europhysics Letters (EPL)* **2007**, *80*, 56004.
(73) Locatelli, E.; Pierno, M.; Baldovin, F.; Orlandini, E.; Tan, Y.; Pagliara, S. Single-File Escape of Colloidal Particles from Microfluidic Channels. *Phys. Rev. Lett.* **2016**, *117*, 038001.
(74) Lin, B.; Meron, M.; Cui, B.; Rice, S. A.; Diamant, H. From Random Walk to Single-File Diffusion. *Phys. Rev. Lett.* **2005**, *94*, 216001.
(75) Locatelli, E.; Baldovin, F.; Orlandini, E.; Pierno, M. Active Brownian Particles Escaping a Channel in Single File. *Phys. Rev. E* **2015**, *91*, 022109.
(76) Kokot, G.; Das, S.; Winkler, R. G.; Gompper, G.; Aranson, I. S.; Snezhko, A. Active Turbulence in a Gas of Self-Assembled Spinners. *Proc. Natl. Acad. Sci. U. S. A.* **2017**, *114*, 12870−12875.
(77) Wensink, H. H.; Dunkel, J.; Heidenreich, S.; Drescher, K.; Goldstein, R. E.; Löwen, H.; Yeomans, J. M. Meso-Scale Turbulence in Living Fluids. *Proc. Natl. Acad. Sci. U. S. A.* **2012**, *109*, 14308−14313.
(78) Vedula, S. R. K.; Leong, M. C.; Lai, T. L.; Hersen, P.; Kabla, A. J.; Lim, C. T.; Ladoux, B. Emerging Modes of Collective Cell Migration Induced by Geometrical Constraints. *Proc. Natl. Acad. Sci. U. S. A.* **2012**, *109*, 12974−12979.
(79) Thampi, S. P.; Doostmohammadi, A.; Shendruk, T. N.; Golestanian, R.; Yeomans, J. M. Active Micromachines: Microfluidics Powered by Mesoscale Turbulence. *Sci. Adv.* **2016**, *2*, No. e1501854.
(80) Liu, C.; Zhou, C.; Wang, W.; Zhang, H. P. Bimetallic Microswimmers Speed Up in Confining Channels. *Phys. Rev. Lett.* **2016**, *117*, 198001.

DOI: 10.1021/acsnano.9b02100
ACS Nano XXXX, XXX, XXX−XXX

(81) Yu, H.; Kopach, A.; Misko, V. R.; Vasylenko, A. A.; Makarov, D.; Marchesoni, F.; Nori, F.; Baraban, L.; Cuniberti, G. Confined Catalytic Janus Swimmers in a Crowded Channel: Geometry-Driven Rectification Transients and Directional Locking. *Small* **2016**, *12*, 5882−5890.
(82) Das, S.; Garg, A.; Campbell, A. I.; Howse, J.; Sen, A.; Velegol, D.; Golestanian, R.; Ebbens, S. J. Boundaries Can Steer Active Janus Spheres. *Nat. Commun.* **2015**, *6*, 8999.
(83) Palacci, J.; Sacanna, S.; Vatchinsky, A.; Chaikin, P. M.; Pine, D. J. Photoactivated Colloidal Dockers for Cargo Transportation. *J. Am. Chem. Soc.* **2013**, *135*, 15978−15981.
(84) Simmchen, J.; Katuri, J.; Uspal, W. E.; Popescu, M. N.; Tasinkevych, M.; Sánchez, S. Topographical Pathways Guide Chemical Microswimmers. *Nat. Commun.* **2016**, *7*, 10598.
(85) Takagi, D.; Palacci, J.; Braunschweig, A. B.; Shelley, M. J.; Zhang, J. Hydrodynamic Capture of Microswimmers into Sphere-Bound Orbits. *Soft Matter* **2014**, *10*, 1784−1789.
(86) Restrepo-Pérez, L.; Soler, L.; Martínez-Cisneros, C. S.; Sánchez, S.; Schmidt, O. G. Trapping Self-Propelled Micromotors with Microfabricated Chevron and Heart-Shaped Chips. *Lab Chip* **2014**, *14*, 1515−1518.
(87) Takatori, S. C.; De Dier, R.; Vermant, J.; Brady, J. F. Acoustic Trapping of Active Matter. *Nat. Commun.* **2016**, *7*, 10694.
(88) Zong, Y.; Liu, J.; Liu, R.; Guo, H.; Yang, M.; Li, Z.; Chen, K. An Optically Driven Bistable Janus Rotor with Patterned Metal Coatings. *ACS Nano* **2015**, *9*, 10844−10851.
(89) Zhou, C.; Zhao, L.; Wei, M.; Wang, W. Twists and Turns of Orbiting and Spinning Metallic Microparticles Powered by Megahertz Ultrasound. *ACS Nano* **2017**, *11*, 12668−12676.
(90) Orozco, J.; Campuzano, S.; Kagan, D.; Zhou, M.; Gao, W.; Wang, J. Dynamic Isolation and Unloading of Target Proteins by Aptamer-Modified Microtransporters. *Anal. Chem.* **2011**, *83*, 7962−7969.
(91) Campuzano, S.; Orozco, J.; Kagan, D.; Guix, M.; Gao, W.; Sattayasamitsathit, S.; Claussen, J. C.; Merkoçi, A.; Wang, J. Bacterial Isolation by Lectin-Modified Microengines. *Nano Lett.* **2012**, *12*, 396−401.
(92) Lin, Z.; Gao, C.; Chen, M.; Lin, X.; He, Q. Collective Motion and Dynamic Self-Assembly of Colloid Motors. *Curr. Opin. Colloid Interface Sci.* **2018**, *35*, 51−58.
(93) Liu, C.; Xu, T.; Xu, L.-P.; Zhang, X. Controllable Swarming and Assembly of Micro/Nanomachines. *Micromachines* **2018**, *9*, 10.
(94) Zöttl, A.; Stark, H. Emergent Behavior in Active Colloids. *J. Phys.: Condens. Matter* **2016**, *28*, 253001.
(95) Bialké, J.; Speck, T.; Löwen, H. Active Colloidal Suspensions: Clustering and Phase Behavior. *J. Non-Cryst. Solids* **2015**, *407*, 367−375.
(96) Aranson, I. S. Collective Behavior in Out-of-Equilibrium Colloidal Suspensions. *C. R. Phys.* **2013**, *14*, 518−527.
(97) Zhang, J.; Luijten, E.; Grzybowski, B. A.; Granick, S. Active Colloids with Collective Mobility Status and Research Opportunities. *Chem. Soc. Rev.* **2017**, *46*, 5551−5569.
(98) Speck, T. Collective Behavior of Active Brownian Particles: From Microscopic Clustering to Macroscopic Phase Separation. *Eur. Phys. J.: Spec. Top.* **2016**, *225*, 2287−2299.
(99) Bricard, A.; Caussin, J.-B.; Desreumaux, N.; Dauchot, O.; Bartolo, D. Emergence of Macroscopic Directed Motion in Populations of Motile Colloids. *Nature* **2013**, *503*, 95−98.

DOI: 10.1021/acsnano.9b02100
ACS Nano XXXX, XXX, XXX−XXX